International Journal of Radiology and Diagnostic Imaging

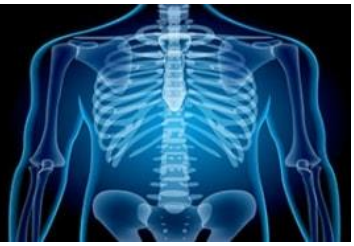

E-ISSN: 2664-4444
P-ISSN: 2664-4436
www.radiologypaper.com
IJRDI 2024; 7(3): 54-61
Received: 18-06-2024
Accepted: 25-07-2024

Ali El-Sayed El-Zayat
Department of Radiodiagnosis Medicine, Faculty of Medicine, Tanta University, Tanta, Egypt

Mohamed Adel El-Tomey
Department of Radiodiagnosis Medicine, Faculty of Medicine, Tanta University, Tanta, Egypt

Mohamed A Alm El-din
Department of Clinical Oncology, Faculty of Medicine, Tanta University, Tanta, Egypt

Mohamed Fathy Dawood
Department of Radiodiagnosis Medicine, Faculty of Medicine, Tanta University, Tanta, Egypt

Corresponding Author:
Ali El-Sayed El-Zayat
Department of Radiodiagnosis Medicine, Faculty of Medicine, Tanta University, Tanta, Egypt

Role of magnetic resonance imaging in prostate cancer

Ali El-Sayed El-Zayat, Mohamed Adel El-Tomey, Mohamed A Alm El-din and Mohamed Fathy Dawood

DOI: https://doi.org/10.33545/26644436.2024.v7.i3a.398

Abstract
Background: Integrating multi-parametric magnetic resonance imaging (MRI) into a program for detection appears to be the most effective method for enhancing the early diagnosis of prostate cancer (P Ca). The objective of this study was to evaluate the utility of MRI in the diagnosis and classification of P Ca.
Methods: This study was conducted on a sample of 30 male patients, aged between 65 and 84 years old, using a cross-sectional descriptive study, with elevated prostate-specific antigen for diagnosis and known P Ca patients for grading, all having no contraindication to MRI. Patients were subjected to MRI examination and Trans-rectal ultrasound guided biopsy.
Results: There was no significant correlation between apparent diffusion coefficient (ADC) and other variables. The best cutoff point of ADC to identify cases with clinically significant lesions was > 0.633 mm^2/s $x10^{-3}$ with 77.3% sensitivity and 62.5% specificity. There was significant difference between the clinically significant and clinically insignificant cases regarding the distribution of the prostate imaging-reporting and data system (PIRADS) categories ($p< 0.001$). There was significant difference between the Gleason score (GS) categories regarding the distribution of the PIRADS categories (P = 0.002).
Conclusion: The trans-rectal ultrasound biopsy is the established clinical standard for definitively diagnosing prostate cancer. MRI plays a crucial role in enhancing the safety of diagnostic procedures. Additionally, it can assist in the process of staging, as well as in the planning of surgery or radiation treatment. Furthermore, the incorporation of multi-parametric MRI and diffusion weighted imaging into a diagnostic program enhances the accuracy of the diagnosis.

Keywords: Magnetic resonance imaging, prostate cancer, Gleason score, apparent diffusion coefficient, PIRADS

Introduction
Prostate cancer, often known as P Ca, is a major global health concern that primarily affects older men. The incidence of this cancer has consistently rated high in global cancer surveys for many years, and its fatality rate is second only to that of lung cancer [1].
P Ca is a slowly progressing cancer that may not show any symptoms over a person's lifespan. Additionally, the histologic prevalence of this disorder can reach as high as 70% in males ages 80 years of age or older. The incidence of this condition increases with age [2].
P Ca is diagnosed differently from other solid organ tumors. Alternatively, the conventional diagnostic approach for prostate cancer (P Ca) involves the utilization of transrectal ultrasound (TRUS) to guide biopsies. This method uses many needles to take samples from various parts of the prostate gland, without prior information about the probable tumor's locations. The patients assigned for this study are males who have not undergone a biopsy before and have prostate-specific antigen (PSA) raised level in their blood and/or abnormal outcomes during a digital rectal examination (DRE). This approach is also suitable for men who are considered to be at a continued high risk of having significant cancers even after previous negative TRUS biopsies, as well as males with low-risk P Ca who are being actively monitored and require repeated sampling of the prostate gland for disease monitoringa [3].
In recent years, magnetic resonance imaging (MPMRI) has the potential to bring about a revolution in the process of developing an alternative diagnostic approach that involves multiparametric P Ca therapy. As part of the triage phase in this pathway, if clinical suspicion has been established, the patient is required to undergo MPMRI examination of the prostate.

Avoiding biopsy can be possible if MPMRI results are negative, whereas positive MPMRI results may indicate the need for targeted biopsy [4]. Among several multi-parametric sequences, DWI is an influential clinical tool that offers functional insights into tissue at a cellular level. The apparent diffusion coefficient (ADC) has demonstrated enhanced accuracy in conjunction with DWI analysis for the identification and localization of P Ca. The truth of this statement is widely acknowledged, with a sensitivity of 82.6% and a specificity of 91.3%. In addition to this, it possesses a percent positive predictive value as well as a hundred percent negative predictive value [5].

In 2015, the Prostate Imaging-Reporting and Data System (PI-RADS) version 2 (PI-RADS v2) was developed. The primary objectives of the second iteration of the PI-RADS were as follows: to establish a uniform and streamlined terminology and content for MPMRI prostate reports; to create assessment categories that succinctly convey the probability of clinically significant prostate cancer (CSPCA); to aid in the identification of patients suitable for biopsies and treatment choices; to define acceptable technical parameters for MPMRI; and to reduce discrepancies in imaging interpretations [6].

There is a strong correlation between higher categories of MRI-based extra prostatic extension (EPE) grading and an increased likelihood of pathologic EPE. The combination of clinical characteristics and MRI grading demonstrated the most accurate diagnostic performance in predicting pathologic EPE [7].

This study objective is to determine whether or not magnetic resonance imaging (MRI) is useful in the diagnosis and classification of P Ca.

Patients and Methods

This study was carried out on a sample of 30 male patients, their age between 65 and 84 years old. The patients had increased levels of PSA for diagnostic purposes and were known to have P Ca for grading. Additionally, all participants had no medical conditions that would prevent them from undergoing MRI. The study was conducted between 2020 and 2021 with approval from the Ethical Committee of Tanta University Hospitals in Tanta, Egypt. The patients provided their informed written permission. The exclusion criteria included patients with contraindications for MRI, including those with implanted magnetic devices, pacemakers, or claustrophobia, as well as individuals with aberrant coagulopathy, local infection, poor general health requiring life support, and severe hepato-renal illness.

Every single patient was subjected to a rigorous process that consisted of getting a comprehensive medical history, carrying out a comprehensive clinical examination, carrying out laboratory testing to assess PSA levels, and carrying out radiographic tests such as ultrasound and MRI.

MRI examination

The use of a 1.5 Tesla magnetic resonance imaging (MRI) scanner that was produced by General Electric (GE) Medical Systems? Each magnetic resonance imaging (MRI) study consisted of three sequences: A T_1-weighted image (TR<800, TE<30, flip angle: 90 degrees), a T_2-weighted image (TR>2000, TE>80, flip angle: 90 degrees), and a diffusion weighted image. The images were acquired in the axial plane using the single-shot echo-planar imaging technique. The application of diffusion encoding gradients was executed using b values ranging from 500 to 1000 s/mm^2. In addition, dynamic contrast enhancement magnetic resonance imaging (DCE-MRI) is used to measure the extent of water molecule diffusion in tissue.

The single-shot echo-planar imaging approach was utilized to capture DW images as they were acquired in the axial plane. The scanning parameters used were a range of 2,740-2,750 for one parameter and 83-85 for another; a slice thickness of 3 mm; a gap of 1 mm between slices; a matrix size of 112 × 110; a FOV of 20 cm; a SENSE factor of 2; and an NSA of 6. Along each of the three orthogonal directions of motion-probing gradients, diffusion-encoding gradients were implemented with three distinct b values: 0 units per millimeter, 600 units per millimeter, and 800 units per millimeter. The generation of ADC maps was accomplished by the use of an automated technique, as each pixel was analyzed separately. The DWI acquisition time was less than 3 minutes. Every completed sequence was evaluated for each patient. The T2WI was initially examined to identify the region of decreased intensity in comparison to the elevated signal intensity of the typical outside zone. In DWI, the presence of tumor was determined based on the presence of localized areas of increased brightness and corresponding areas of decreased brightness on the ADC map, in comparison to the surrounding tissue of the prostate gland. Due to the fact that an ADC map was automatically constructed for each slice, mapping the ADC values pixel by pixel, the grey value of the pixel was directly proportional to the ADC values (mm^2/s x10^{-3}). The value was computed using the aforementioned equation. The results obtained by T2WI were compared to those obtained from the combination of T2WI and DWI.

Trans-rectal ultrasound guided biopsy protocol:

Biopsies are performed using sextant TRUS guidance on patients whose PSA levels are greater than 4 ng/ml. The MRI test was carried out either before to the TRUS biopsy or at a minimum of three weeks after the TRUS biopsy. Evaluation of the histology by a pathologist with extensive experience was performed on the specimen.

Gleason grading: It is a reliable indicator of the probability of survival in men with prostate cancer. All of the primary and secondary patterns are added together to form the GS, which has a range of 2 to 10. It has been widely recognized that patients with a GS of 7 or higher are at a higher risk for EPE and biochemical recurrence [8].

Statistical analysis

Utilizing the SPSS v26 program (IBM Inc., Chicago, Illinois, United States of America), the statistical analysis was carried out. Histograms and the Shapiro-Wilks test were utilized in order to determine whether or not the data distribution in question was normal. With the help of an unpaired Student's t-test, the mean and standard deviation (SD) of the quantitative parametric variables were provided, and a comparison was made between the two groups. Both the median and the interquartile range (IQR) were supplied for the quantitative non-parametric data, and the Mann Whitney test was utilized to analyze the data. The qualitative variables were analyzed using the Chi-square test or Fisher's exact test, depending on the circumstances. The frequency and percentage (%) values were displayed for the

qualitative variables. The equation for Pearson's correlation coefficient was utilized in order to determine the degree of correlation that exists between the various variables. In order to evaluate the diagnostic performance in terms of sensitivity, specificity, positive predictive value (PPV), and negative predictive value (NPV), the ROC curve was applied. To be considered statistically significant, a two-tailed P value that was lower than 0.05 was required.

Results

Age, PSA, affected prostatic zones, GS, PIRADS, maximum transverse diameter of the detected lesion, EPE, T, N and M staging, ADC value and clinical significance of the prostatic lesions were enumerated in this table. Table 1.

Table 1: Age, PSA, affected prostatic zones, GS and PIRADS, maximum transverse diameter of the detected lesion, EPE, T, N and M staging, ADC value and clinical significance of the prostatic lesions of the studied cases

		N = 30
Age (years)		73.9±6.52
PSA (ng/ml)		21.45(7.6-609.2)
Affected prostatic zones	Peripheral zone	14(46.7%)
	Central zone	5(16.7%)
	Transitional zone	8(26.7%)
	Infiltrative lesion (> 1 zone)	3(10.0%)
GS	3+3	4(13.3%)
	3+4	4(13.3%)
	4+3	8(26.7%)
	4+4	8(26.7%)
	4+5	6(20.0%)
PIRADS	PIRADS 2	4(13.3%)
	PIRADS 3	7(23.3%)
	PIRADS 4	13(43.3%)
	PIRADS 5	6(20.0%)
Maximum transverse diameter (mm)		23(4-35)
EPE		13(43.3%)
T stage	1	13(43.3%)
	2	4(13.3%)
	3A	4(13.3%)
	3B	4(13.3%)
	4	5(16.7%)
N stage	N0	24(80%)
	N1	6(20%)
M stage	M0	30(10%)
	M1	0(0%)
ADC (mm^2/s x10^{-3})		0.698±0.093
Clinically significant		22(73.3%)

Data are presented as mean ± SD or median (IQR) or frequency (%). PSA: Prostate-specific antigen, PIRADS: Prostate imaging reporting and data system, GS: Gleason score, ADC: Apparent diffusion coefficient, EPE: Extra prostatic extension. There was significant difference between the clinically significant and clinically insignificant cases regarding the distribution of the PIRADS categories (p< 0.001) and there was no significant difference between the clinically significant and clinically insignificant cases regarding the ADC (P = 0.510). Table 2.

Table 2: Relation between PIRADS category and clinical significance and comparison of ADC values according to the clinical significance of the lesions

	Clinically insignificant (n=8)	**Clinically significant (n=22)**	**P**
PIRADS 2	4(50%)	0(0.0%)	< 0.001*
PIRADS 3	4(50%)	3(13.6%)	
PIRADS 4	0(0.0%)	13(59.1%)	
PIRADS 5	0(0.0%)	6(27.3%)	
ADC (mm^2/s x10^{-3})	0.679±0.100	0.705±0.092	0.510

Data are presented as mean ± SD or frequency (%). * Significant (p value< 0.05). ADC: Apparent diffusion coefficient, PIRADS: Prostate imaging reporting and data system.

There was no significant correlation between ADC and other variables. Table 3.

Table 3: Correlation between ADC values with other variables

	ADC (mm^2/s x10^{-3})	
	Rs	**P**
PSA	-0.041	0.830
PIRADS	0.060	0.754
Maximum transverse diameter	0.233	0.215

Rs: spearman correlation, PSA: prostate-specific antigen, PIRADS: prostate imaging reporting and data system.
Regarding the ADC, there was no significant difference between the GS categories and affected zone. Table 4.

Table 4: Relation between GS and affected zones and ADC

		ADC (mm^2/s $x10^{-3}$)	P
GS	3+3 (N=4)	0.72±0.12	0.678
	3+4 (N=4)	0.64±0.07	
	4+3 (N=8)	0.70±0.08	
	4+4 (N=8)	0.72±0.10	
	4+5 (N=6)	0.68±0.10	
Affected zones	Peripheral zone (N=14)	0.70±0.08	0.976
	Central zone (N=5)	0.7±0.11	
	Transitional zone (N=8)	0.69±0.11	
	Infiltrative lesions (N=3)	0.70±0.10	

Data are presented as mean ± SD or frequency (%). ADC: Apparent diffusion coefficient, GS: Gleason score.

There was significant difference between the GS categories regarding the distribution of the PIRADS categories (P = 0.002). Table 5.

Table 5: Relation between GS and PIRADS

	GS					P
	3+3	3+4	4+3	4+4	4+5	
PIRADS 2	3(75.0%)	1(25.0%)	0(0.0%)	0(0.0%)	0(0.0%)	0.002*
PIRADS 3	1(25.0%)	3(75.0%)	2(25.0%)	1(12.5%)	0(0.0%)	
PIRADS 4	0(0.0%)	0(0.0%)	5(62.5%)	5(62.5%)	3(50.0%)	
PIRADS 5	0(0.0%)	0(0.0%)	1(12.5%)	2(25.0%)	3(50.0%)	

Data are presented as frequency (%). * Significant (p value< 0.05). PIRADS: prostate imaging reporting and data system, GS: Gleason score.

The best cutoff point of ADC to identify cases with clinically significant lesions was > 0.633 mm^2/s $x10^{-3}$ with 77.3% sensitivity and 62.5% specificity. Figure 1.

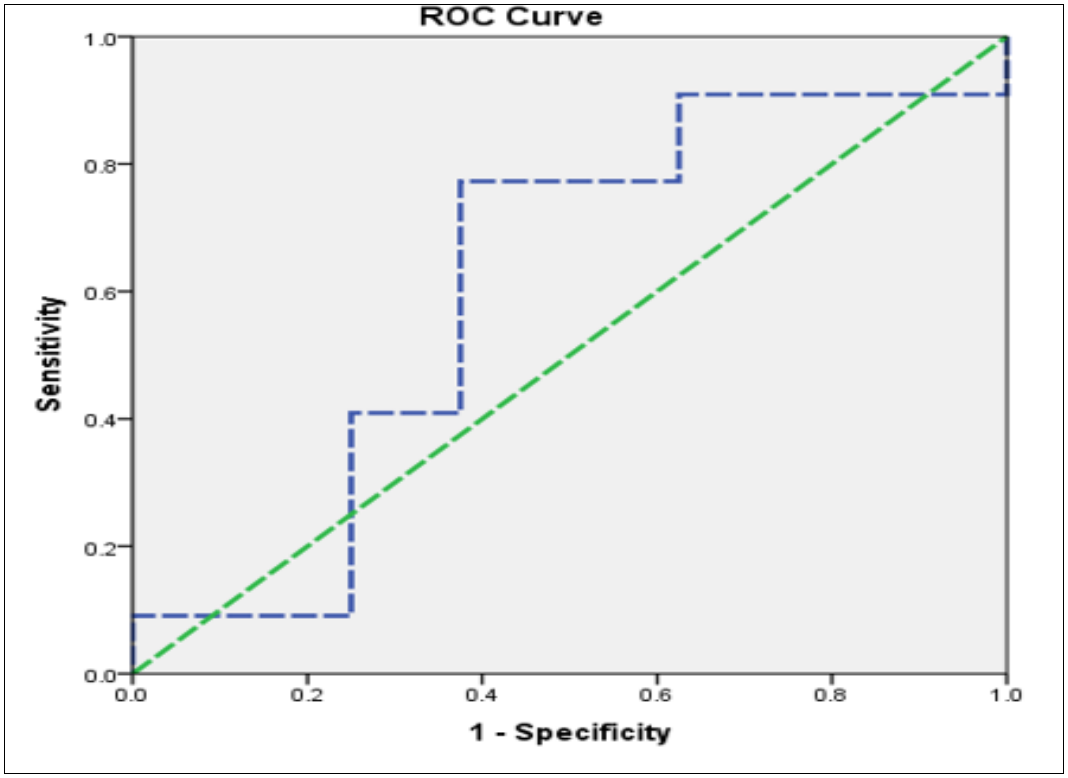

Fig 1: ROC curve of ADC value to identify clinically significant lesions

Case 1: 72 years old male patient. Figure 2.

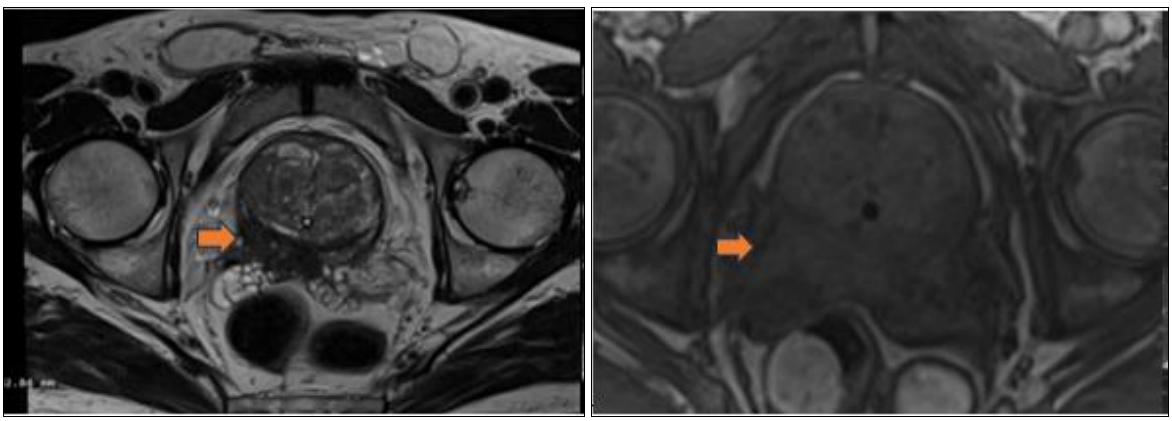

A **B**

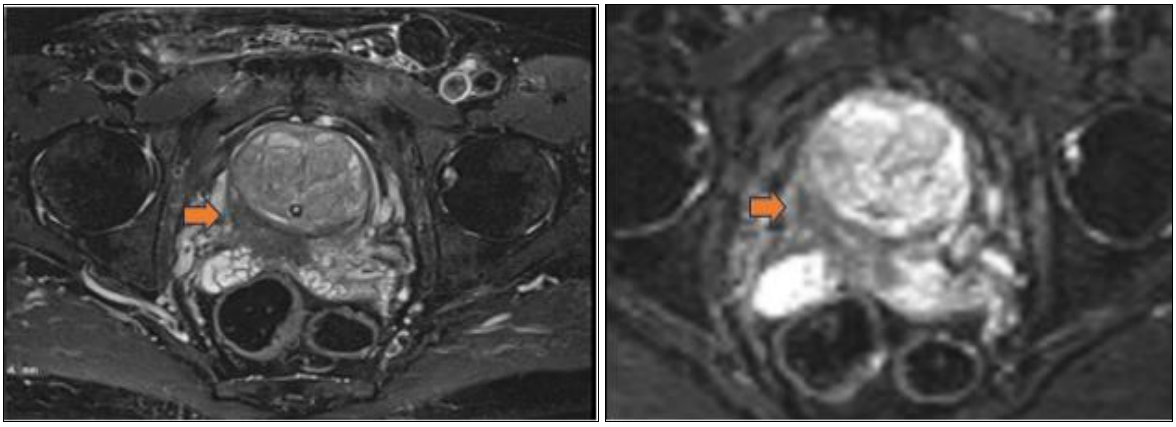

C **D**

Fig 2: (A) The prostate is markedly enlarged in size measuring about 5.9x6.7x7.2 cms at its maximum AP, TS and CC dimensions respectively with total volume about 140 cc. uplifting the bladder base, (B) Axial T2 showing peripheral zone large ill-defined area of low T2WI signal seen at the center and all the right posterolateral aspect of the gland crossing the midline. It is seen invading the capsule, both seminal vesicles more on the right side which shows low T2 signal with thickening of the neurovascular bundle at 7 O'clock denoting infiltration with soft tissue sheets seen extending along the right lateral neurovascular bundle likely Perineural spread, (C) Restriction in DWI study and low ADC value about 0.423 x 10^{-3}Amm, (D) Dynamic contrast shows early arterial enhancement and washout in the dynamic sequences PIRADS 5

Case 2: 68 years old male patient. Figure 3.

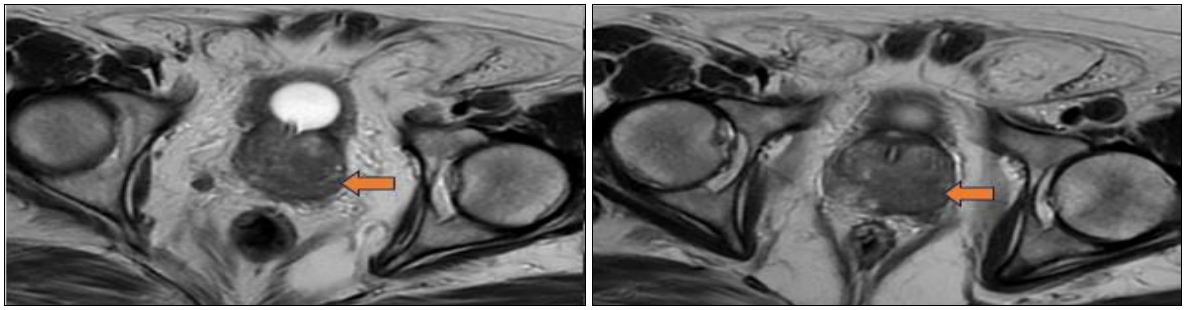

A

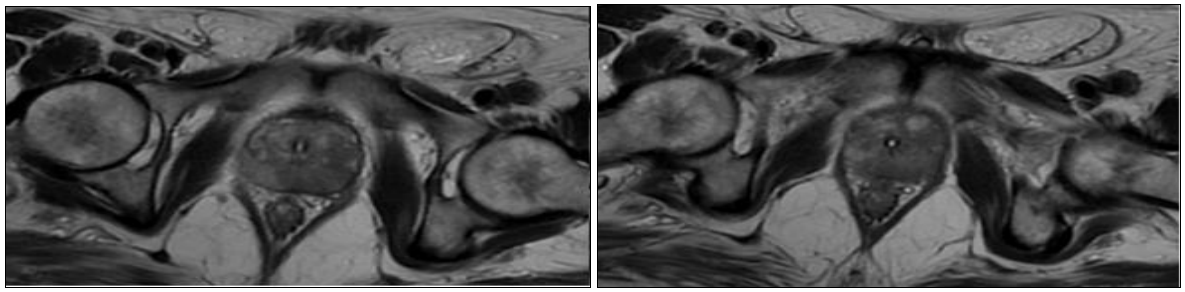

B

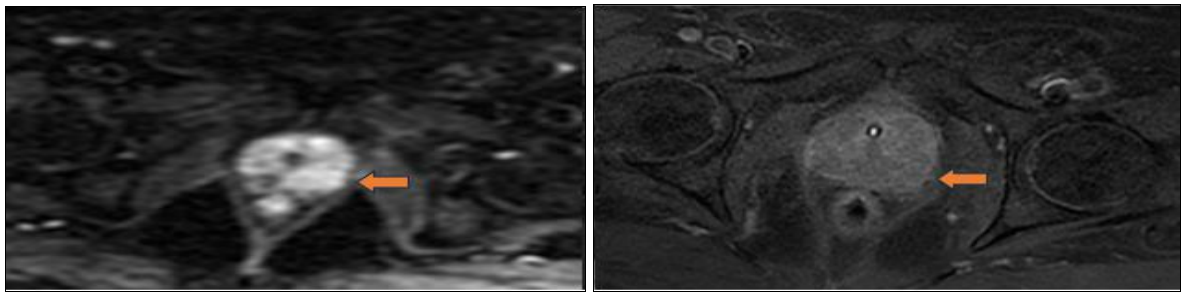

C

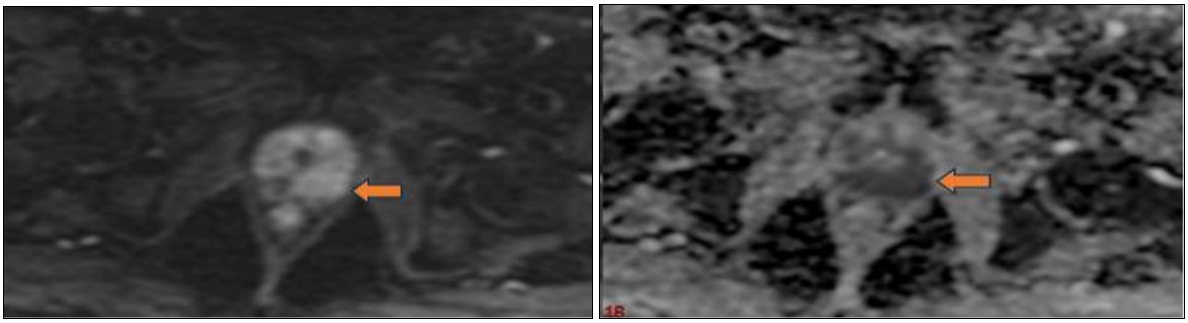

D

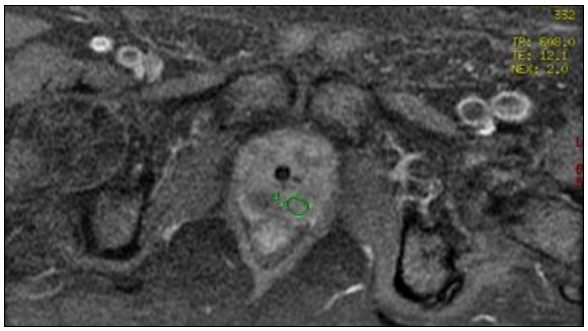

E

Fig 3: (A) The prostate is markedly enlarged in size (4x4.5x6cm) uplifting the bladder base, (B) Peripheral zone shows Well-defined ovoid shaped left sided T2 hypointense lesion averages 2.3x2.8x4cm with violating of the related central zones as well involving (PZa, PZpl, PZpm, CZ and TZp) with suspected implication of the left neurovascular bundle, (C) Restriction in DWI study and low intense signal in ADC, (D) Dynamic contrast enhancement shows positive homogenous enhancement of the focal lesion PIRADS 5, (E) Enlarged right peri-prostatic LN averages 6mm shows restricted diffusion likely metastatic

Case 3: 62 years old male patient. Figure 4.

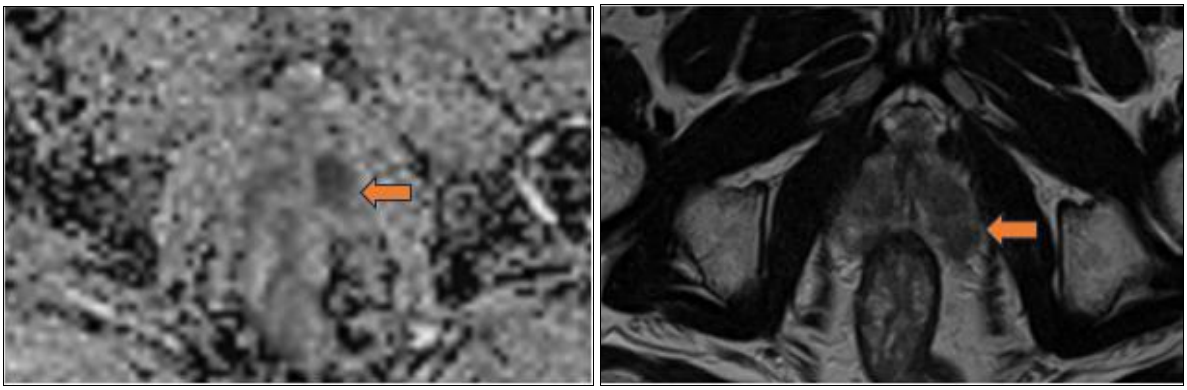

A B

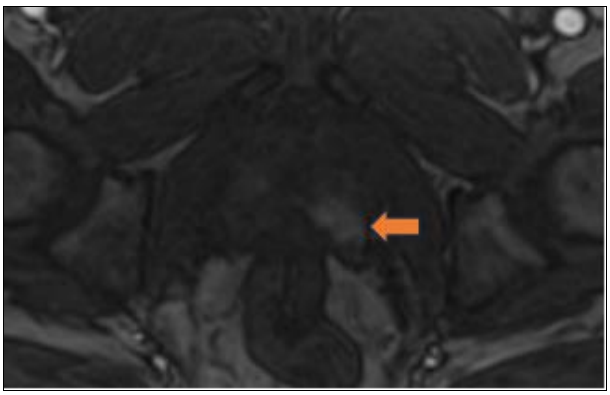

C

Fig 4: (A) The prostate is enlarged in size measures (4.4x5.6x4.9cm), (B) Peripheral zone shows Well-defined ovoid shaped left sided T2 hypointense lesion averages 17x8mm involving (PZpl, PZpm), (C) Restriction in DWI study and low intense signal in ADC. (D) Dynamic contrast enhancement shows positive homogenous enhancement of the focal lesion PIRADS

Discussion

P Ca is a prevalent form of cancer in older men and is a major factor contributing to cancer-related deaths. [9].

In the current study, the GS was 6 (3+3) in 4 cases (13.3%), score 7 (3+4) in 4 cases (13.3%), score 7 (4+3) in 8 cases (26.7%), score 8 (4+4) in 8 cases (26.7%) and score 9 (4+5) in 6 cases 20%. In another study that by Wang *et al.* [10] where 462 cases were included. Forty-three cases (9.31%) were having GS of <7, while 178 cases (38.52%) were having score of 7. In addition, 153 cases (33.12%) and 88 cases (19.05%) were having scores equal and more than 8 respectively. In the study conducted by Ali *et al.* [11] that included 30 patients with prostate cancer, Out of them 2 have a Gleason score (GS) of 6 and 28 their GS is 7 or higher. Specifically, there are 9 cases with a GS of 7, 16 cases with a GS of 8, and 1 case with a GS of 9. The median value of GS is 8.

In the current study, EPE was reported in 13 cases (43.3%). This agreed with the results of AbdelMaboud *et al.* [12] that included 32 cancer prostate lesions, Extracapsular extension, without invasion of nearby organs, was identified in 5 cases. Asymmetry of the neurovascular bundle was observed in one of the cases, tumor envelopment of the neurovascular bundle was observed in another case, abnormalities of the prostate capsule were observed in two of the cases, and the recto prostatic angle was completely obliterated in one of the cases.

In this study, patients were categorized based on the clinical significance of their cases. The findings reveal that 73.3% of patients had clinically significant malignancy, defined as a GS of 7 or higher, or EPE. This percentage was almost equal to AbdelMaboud *et al.* [13] showed that the percentage of clinically significant prostate lesion was 73%.

Regarding the TNM classification, there was 4 cases (13.3%) with stage T3a stage, 4 cases (13.3%) with stage T3b and 5 cases (16.7%) with stage T4. Positive nodal affection was shown in 6 cases (20%). According to the study by ALI *et al.* [14] reported that lesion was infiltrating the base of the urinary bladder or encroaching onto the wall of the rectum (stage T4). This was the fourth stage of the lesion. A total of five cases, or 16.6% of the overall number of cases, displayed evidence of extracapsular enlargement (stage T3a), while three cases, or 10% of the total, had seminal vesicle invasion (stage T3b).

Out of the total number of cases, 5 individuals (16.6%) were found to have regional lymph node metastases, specifically classified as stage N1, 11 (36.6%) were diagnosed with bone metastases at stage M1b. The most prevalent category in the current investigation was PIRADS 4, which was found in 43.3% of the instances. This was followed by PIRADS 3, which was found in 23.3% of the cases, then PIRADS 5, which was found in 20% of the cases, and finally PIRADS 2, which was found in 13.3% of the cases. There was a significant and meaningful difference in the distribution of PIRADS classification based on the clinical importance. All the cases with PIRADS 2 were clinically insignificant while all the cases with PIRADS 4 and 5 were clinically significant. PIRADS 5 showed the highest diagnostic accuracy in detection of clinically significant lesions with 72.3% sensitivity, 100% specificity, 100% PPV, 83.1% NPV and 86.7% total accuracy. Ali *et al.* [11] showed that the utilization of PI-RADS version 2 has greatly enhanced the accuracy in identifying clinically relevant malignancy during the diagnostic process. PI-RADS version 2 demonstrated a sensitivity of 80% in detecting malignant lesions, both significant and insignificant, with regard to a PIRADS score larger than 3 as a strong signal for malignancy. The obtained outcomes are rational and satisfactory if compared to the results of Ahmed *et al.* [15] study, which demonestrate a sensitivity and specificity of 93% and 41% respectively.

In this investigation, ADC mean of the included lesions was 0.698±0.093 mm^2/s $x10^{-3}$ with range between 0.595 and 0.884 mm^2/s $x10^{-3.}$ The mean ADC value in the clinically insignificant lesions was 0.679±0.100 mm^2/s $x10^{-3}$ that was lower as compared to 0.705±0.092 mm^2/s $x10^{-3,}$ but it didn't reach a statistically significant value. The best cutoff point of ADC to differentiate the cases with significant prostate lesions was > 0.633 mm^2/s $x10^{-3}$ with 77.3% sensitivity and 62.5% specificity. This was in accordance with AbdelMaboud *et al.* [12] showed that the ADC value was found to be lower in the prostate that was cancerous in comparison to the prostate that was healthy. The specific values for the histopathologically confirmed benign peripheral zone were 1.484 ±0.289 · mm^2/s $x10^{-3}$, while the histopathologically proven malignant prostate had a value of 0.737 ±0.154 mm^2/s $x10^{-3}$ according to the histological findings. The average axial displacement coefficients (ADCs) for cases of urinary bladder wall invasion were 0.963±0.155 mm^2/s $x10^{-3}$, while the ADCs for the normal bladder wall were 1.517±0.103 mm^2/s $x10^{-3}$. In the study conducted by Pepe *et al.* [16] The diagnostic accuracy of ADC (with a cut-off of 0.747) compared to PIRADS score ≥3 in diagnosing GS ≥7 was as follows: sensitivity 84% vs. 63.6%, specificity 93.5% vs. 77.4%, positive predictive value 61.5% vs. 30.7%, and negative predictive value 85.2% vs. 77.5%. Additionally, the ADC had a higher accuracy in terms of overall diagnostic performance (80% vs. 36.3%). The AUC ROC is presented for the comparison between ADC with a cutoff value of 0.747×10^{-3} and PI-RADS score of 3 or higher in the P Ca diagnosis with a GS of 7 or higher. The present investigation found no statistically significant variation in the ADC results of men between the cases based on the GS. This agreed with Woo *et al.* [17] discovered that despite the fact that the ADC ratio between the tumor and the bladder had the greatest AUC of all the ADC ratios that were investigated, it was not significantly better than the mean ADC (AUC = 0.790 versus AUC = 0.794, P = 0.803). In the current investigation, there was a slight non-statistically significant straight forward correlation between ADC and age, PIRADS and Maximum transverse diameter. This disagreed with Tamada *et al.* [18] found Men between the ages of 60 and 89 have greater ADC values in comparison to middle-aged males (40-59 years) and young males (20-39 years). The ADC values for men of advanced age are 1.74±0.25 × 10^{-3} mm^2/s, whereas for middle-aged men they are 1.37±0.18 × -3 mm^2/s, and for young men they are 1.63±0.26 × 10^{-3} mm^2/s.

The primary limitations that potentially reduce the power of the outcomes gained are the limited size of sample and the fact that the study was carried out at a single center. Also, this is a cross-sectional clinical study without longitudinal prospective data, this could decrease the power of the obtained results.

Conclusion

The conclusive diagnosis of prostate cancer is typically made by trans-rectal ultrasound (TRUS) biopsy, which is

considered the clinical standard. Nevertheless, this particular TRUS guided biopsy method is prone to significant sample error, potentially resulting in the failure to detect up to 30% of cancers. Additionally, it may also lead to an underestimating of the Gleason grade, particularly in tumors placed in the anterior region. The utilization of MRI is crucial in enhancing the safety of diagnostic procedures and reducing the likelihood of problems. In addition to this, it can be of use in the process of staging, as well as in the planning of surgical procedures or radiation therapy. The integration of MP MRI and DWI into diagnostic software enhances the diagnostic accuracy.

Financial support and sponsorship: Nil.

Conflict of Interest: Nil.

References

1. Shan Y, Chen X, Liu K, Zeng M, Zhou J. Prostate cancer aggressive prediction: preponderant diagnostic performances of intravoxel incoherent motion (IVIM) imaging and diffusion kurtosis imaging (DKI) beyond ADC at 3.0 T scanner with Gleason score at final pathology. Abdominal Radiology. 2019;44:3441-3452.
2. Popat PB, Maheshwari S, Sable NP, Thakur M, Katdare A. Multiparametric MRI approach to prostate cancer with a pictorial essay on PI-RADS. Indian Journal of Urology. 2019;20:200-210.
3. Rothwax JT, George AK, Wood BJ, Pinto PA. Multiparametric MRI in biopsy guidance for prostate cancer: fusion-guided. Biomedical Research International. 2014;50:600-650.
4. Padhani AR, Weinreb J, Rosenkrantz AB, Villeirs G, Turkbey B, Barentsz J, *et al*. Prostate Imaging-Reporting and Data System Steering Committee: PI-RADS v2 status update and future directions. European Urology. 2019;75:385-396.
5. Liau J, Goldberg D, Arif-Tiwari H. Prostate cancer detection and diagnosis: role of ultrasound with MRI correlates. Current Radiology Reports. 2019;7:1-12.
6. Lopci E, Saita A, Lazzeri M, Lughezzani G, Colombo P, Buffi NM, *et al.* 68Ga-PSMA positron emission tomography/computed tomography for primary diagnosis of prostate cancer in men with contraindications to or negative multiparametric magnetic resonance imaging: A prospective observational study. Journal of Urology. 2018;200:95-103.
7. Gaur S, Harmon S, Rosenblum L, Greer MD, Mehralivand S, Coskun M, *et al.* Can apparent diffusion coefficient values assist PI-RADS version 2 DWI scoring? A correlation study using the PI-RADS v2 and International Society of Urological Pathology Systems. American Journal of Roentgenology. 2018;211:60-30.
8. Stark JR, Perner S, Stampfer MJ, Sinnott JA, Finn S, Eisenstein AS, *et al.* Gleason score and lethal prostate cancer: Does 3+4= 4+3? Journal of Clinical Oncology. 2009;27:300-350.
9. Khodabandeh M. Prostate cancer and quality of life in the elderly: A literature review. Egyptian Journal of Radiology and Nuclear Medicine. 2024;189:22-29.
10. Wang Y, Chen W, Hu C, Wen X, Pan J, Xu F, *et al.* Albumin and fibrinogen combined prognostic grade predicts prognosis of patients with prostate cancer. Journal of Cancer. 2017;80:39-44.
11. Ali WI, Hammad MI, Alshazly TMSA. Role of multi-parametric magnetic resonance imaging (MRI) in assessment of malignant prostatic lesions. Egyptian Journal of Hospital Medicine. 2019;75:200-300.
12. AbdelMaboud NM, Elsaid HH, Aboubeih EA. The role of diffusion-weighted MRI in evaluation of prostate cancer. Egyptian Journal of Radiology and Nuclear Medicine. 2014;45:231-236.
13. AbdelMaboud NM, Elsaid HH, Aboubeih EA. The role of diffusion-weighted MRI in evaluation of prostate cancer. The Egyptian Journal of Radiology and Nuclear Medicine. 2014;45:231-236.
14. Ali WI, Hammad MI, Alshazly TMSA. Role of Multi-Parametric Magnetic Resonance Imaging (MRI) in Assessment of Malignant Prostatic Lesions. The Egyptian Journal of Hospital Medicine. 2019;75:3099-3106.
15. Ahmed HU, Bosaily AE-S, Brown LC, Gabe R, Kaplan R, Parmar MK, *et al.* Diagnostic accuracy of multi-parametric MRI and TRUS biopsy in prostate cancer (PROMIS): A paired validating confirmatory study. Lancet. 2017;389:815-822.
16. Pepe P, D'Urso D, Garufi A, Priolo G, Pennisi M, Russo G, *et al.* Multiparametric MRI apparent diffusion coefficient (ADC) accuracy in diagnosing clinically significant prostate cancer. *In Vivo*. 2017;31:415-418.
17. Woo S, Kim SY, Cho JY, Kim SH. Preoperative evaluation of prostate cancer aggressiveness: using ADC and ADC ratio in determining Gleason score. American Journal of Roentgenology. 2016;207:114-120.
18. Tamada T, Sone T, Toshimitsu S, Imai S, Jo Y, Yoshida K, *et al.* Age-related and zonal anatomical changes of apparent diffusion coefficient values in normal human prostatic tissues. Journal of Magnetic Resonance Imaging. 2008;27:552-556.

How to Cite This Article
El-Zayat AES, El-Tomey MA, El-din MAA, Dawood. Role of Magnetic Resonance Imaging in Prostate Cancer. International Journal of Radiology and Diagnostic Imaging. 2024;7(3):54-61.